

A Perturbation Method for the $T - \Omega$ Geometric Eddy-Current Formulation

Lorenzo Codecasa¹, Patrick Dular², Ruben Specogna³, and Francesco Trevisan³

¹Politecnico di Milano, Dipartimento di Elettronica ed Informazione, 20133 Milano, Italy

²Université de Liège, F.R.S.-FNRS, ACE, Department of Electrical Engineering and Computer Science, 4000 Liège, Belgium

³Università di Udine, Dipartimento di Ingegneria Elettrica, Gestionale e Meccanica (DIEGM), 33100 Udine, Italy

A perturbation method for the $T - \Omega$ geometric formulation to solve eddy-current problems is introduced. The proposed formulation is applied to the feasibility design of a nondestructive evaluation device suitable to detect “long” longitudinal flaws in hot steel bars.

Index Terms—Cell method (CM), discrete geometric approach (DGA), eddy-currents, finite integration technique (FIT), perturbation method.

I. INTRODUCTION

IN ELECTROMAGNETIC nondestructive methodologies, based on eddy-currents, it is usual procedure to detect the presence of a defect in a conducting medium from the difference between a pair of field configurations, where the defect is present (*defected* configuration) and absent (*undefected* configuration), respectively. Since the effect of the defect modifies only slightly the defected configuration, the abrupt difference between the numerical solutions from a defected and an undefected field configurations yields to cancellation errors; To avoid this problem, perturbation methods have been developed and they are profitably used in finite elements, [1], [2].

In this paper, we will develop a perturbation method within a $T - \Omega$ discrete formulated eddy-currents problem, where a finite dimensional system of equations involving the circulation of the electric vector potential (T) and a magnetic scalar potential (Ω) is deduced by means of the so called *discrete geometric approach* (DGA) [3]–[6]. This method provides an alternative with respect to the classical Galerkin method in finite elements. DGAs put the emphasis on the geometric structure behind Maxwell’s equations and they made visible how the basic laws of eddy-currents—and in general of electromagnetism—can be stated directly in algebraic form, in terms of circulations and fluxes of the related field quantities, plus the discrete counterparts of the constitutive relations.

As an application of remarkable industrial interest, we will apply the discrete perturbation method for $T - \Omega$ formulation to the detection of surface defects that can be present during the hot mill rolling process of the steel bars with circular cross-section (with a diameter from 8 to 80 mm, a speed from 5 to 100 m/s and a temperature from 800 °C to 1200 °C). The defects considered have a depth ranging from 0.1 mm to 2 mm and, even though they have quite different shapes and sizes, they generally correspond to an interruption of the material continuity (also from the electrical point of view) and lay along an almost radial

direction. We will concentrate on long surface defects having an axial length from a meter to tens of meters, where, so far, only few practical working solutions have been proposed.

II. $T - \Omega$ GEOMETRIC FORMULATION

The domain of interest D of the eddy-current problem, has been partitioned into a source region D_s , in a passive conductive region D_c , and the air region D_a .

We cover the domain D with a tetrahedral mesh forming the primal simplicial complex \mathcal{K} whose oriented geometric elements are nodes n , edges e , faces f and volumes v . The interconnections of complex \mathcal{K} are described with incidence matrices: \mathbf{G} between edges e and nodes n , \mathbf{C} between faces f and edges e and \mathbf{D} between volumes v and faces f .

By means of the barycentric subdivision of \mathcal{K} , a dual complex \mathcal{B} is constructed [3], whose geometric elements are volumes v_B , faces f_B , edges e_B and nodes n_B in a one-to-one correspondence (duality) with the geometric elements of \mathcal{K} , respectively. The matrices $\mathbf{G}_B = \mathbf{D}^T$, $\mathbf{C}_B = \mathbf{C}^T$ and $\mathbf{D}_B = -\mathbf{G}^T$ describe the mutual interconnections between the geometric elements of \mathcal{B} .

Next, we consider the integrals of a field quantity with respect to an oriented geometric element of \mathcal{K} and \mathcal{B} ; The arrays they form are referred to as degrees of freedom (DoF) arrays [3], [5] and they will be denoted in boldface type:

- Φ denotes the array of magnetic induction fluxes, where each flux is associated with a face $f_B \in D$;
- \mathbf{F} is the array of magneto-motive forces (m.m.f.s) associated with $e \in D$;
- \mathbf{I} is the array of electric currents associated with $f \in D_c$;
- \mathbf{U} is the array of electro-motive forces (e.m.f.s) along edges $e_B \in D$;
- Finally, in the source region D_s , the array \mathbf{I}_s of known source currents is considered.

With symbol $(\bullet)_x$, with $x \in \{f, e, n, f_B, e_B\}$, we denote the component of an array indexed by x .

According to the DGA, Maxwell’s laws can be written *exactly* as balance equations involving the Dofs arrays of the complex \mathcal{B} or \mathcal{K} . Therefore, in the frequency domain, Gauss’ magnetic law and Faraday’s law can be written, respectively, as

$$\begin{aligned} \mathbf{G}^T \Phi &= \mathbf{0} & (a) \\ \mathbf{C}^T \mathbf{U} &= -i\omega \Phi & (b) \end{aligned} \quad (1)$$

Manuscript received December 18, 2009; accepted February 10, 2010. Current version published July 21, 2010. Corresponding author: R. Specogna (e-mail: ruben.specogna@uniud.it).

Color versions of one or more of the figures in this paper are available online at <http://ieeexplore.ieee.org>.

Digital Object Identifier 10.1109/TMAG.2010.2043932

with respect to \mathcal{B} . With respect to the restrictions of \mathcal{K} in D_c and D_s , in order to satisfy continuity law identically

$$\begin{aligned} \mathbf{D}_c \mathbf{I} &= \mathbf{0} & (a) \\ \mathbf{D}_s \mathbf{I}_s &= \mathbf{0} & (b) \end{aligned} \quad (2)$$

we introduce the arrays \mathbf{T} and \mathbf{T}_s of the circulations of the electric vector potential \mathbf{T} along the edges $e \in D_c$ and $e \in D_s$, respectively, such that

$$\begin{aligned} \mathbf{C}_c \mathbf{T} &= \mathbf{I} & (a) \\ \mathbf{C}_s \mathbf{T}_s &= \mathbf{I}_s & (b) \end{aligned} \quad (3)$$

hold;¹ matrices \mathbf{D}_c and \mathbf{D}_s account for the incidence between the pairs (v, f) in D_c and D_s , while \mathbf{C}_c and \mathbf{C}_s account for the incidence between the pairs (f, e) in D_c and D_s , respectively. The array \mathbf{T}_s is assumed here as known. Ampère's balance law at discrete level yields

$$\begin{aligned} \mathbf{C}_c \mathbf{F}_c &= \mathbf{I} & (a) \\ \mathbf{C}_s \mathbf{F}_s &= \mathbf{I}_s & (b) \\ \mathbf{C}_a \mathbf{F}_a &= \mathbf{0} & (c) \end{aligned} \quad (4)$$

where subscripts c, s and a denote a subarray or a submatrix associated with the geometric elements $e, (f, e)$ in D_c, D_s and D_a , respectively. From the definition of \mathbf{T}, \mathbf{T}_s , (4) is equivalent² to

$$\begin{aligned} \mathbf{F}_c &= \mathbf{G}_c \boldsymbol{\Omega}_c + \mathbf{T} \\ \mathbf{F}_s &= \mathbf{G}_s \boldsymbol{\Omega}_s + \mathbf{T}_s \\ \mathbf{F}_a &= \mathbf{G}_a \boldsymbol{\Omega}_a \end{aligned} \quad (5)$$

where we introduced an array $\boldsymbol{\Omega}$ of magnetic scalar potentials associated with the nodes $n \in D$ whose restrictions to D_c, D_s and D_a yield the subarrays $\boldsymbol{\Omega}_c, \boldsymbol{\Omega}_s$ and $\boldsymbol{\Omega}_a$, respectively; Subscripts c, s and a denote a subarray or a submatrix associated with the geometric elements $n, (e, n)$ in D_c, D_s and D_a , respectively. The interface conditions that avoid the current to flow outside region D_c are taken into account by considering $T = 0, \forall e \in \partial D_c$. In this way, $(\mathbf{I})_f = 0, \forall f \in \partial D_c$ holds.

For the sake of simplicity, we assume that the D_c region does not contain holes.³ In the case D_c contains holes, the m.m.f.s along cycles contained in D_a cannot be described completely by the magnetic scalar potential alone. In this case, the *thick cuts* [8], [9] have to be found and for each thick cut a nonlocal Faraday' law [8], [9] has to be written. One additional unknown per thick cut is added and all of them represent a set of linearly independent currents in D_c .

The discrete counterparts of the constitutive laws must be considered in addition to the discrete formulated laws

$$\begin{aligned} \boldsymbol{\Phi} &= \boldsymbol{\mu} \mathbf{F} & \text{in } D & (a) \\ \mathbf{U}_c &= \boldsymbol{\rho} \mathbf{I} & \text{in } D_c & (b) \end{aligned} \quad (6)$$

where the square matrices $\boldsymbol{\mu}$ and $\boldsymbol{\rho}$ can be efficiently calculated in a pure geometric way for the pair of complexes \mathcal{K}, \mathcal{B} as de-

¹We recall that $\mathbf{D}_x \mathbf{C}_x = \mathbf{0}$ hold for $x \in \{c, s\}$.

²We recall that $\mathbf{C}_x \mathbf{G}_x = \mathbf{0}$ holds for $x \in \{c, s, a\}$.

³Namely, the first Betti number of the D_c region is zero. Thus, D_c is simply-connected or contains cavities.

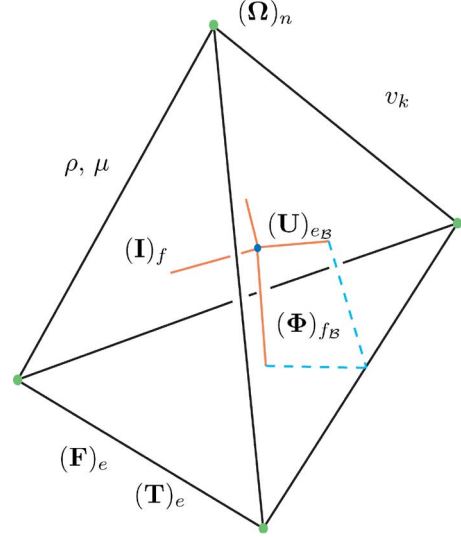


Fig. 1. The geometric elements of \mathcal{B} or \mathcal{K} are shown for a single tetrahedron v_k . The association of integral variables to the corresponding geometric elements is shown in addition. Resistivity and permeability ρ, μ are uniform in each v_k .

scribed in [10] under the hypothesis of element wise uniform distributions of the fields and of the permeability μ and resistivity ρ within each tetrahedron of \mathcal{K} ; Moreover, the linearity of all the media is assumed.

By substituting (6a), (6b), and (5) in (1a), the algebraic equations corresponding to the nodes in D are obtained. By substituting (6a), (6b), and (5) in (1b) the algebraic equations corresponding to edges in D_c are derived. The final algebraic system, having \mathbf{T} and $\boldsymbol{\Omega}$ as unknown DoFs arrays, can be written as

$$\begin{aligned} (\mathbf{G}_c^T \boldsymbol{\mu} \mathbf{G}_c \boldsymbol{\Omega})_n &= 0, & \forall n \in D_a \\ (\mathbf{G}_s^T \boldsymbol{\mu} \mathbf{G}_s \boldsymbol{\Omega})_n &= -(\mathbf{G}_s^T \boldsymbol{\mu}_s \mathbf{T}_s)_n, & \forall n \in D_s \\ (\mathbf{G}_c^T \boldsymbol{\mu} \mathbf{G}_c \boldsymbol{\Omega})_n + (\mathbf{G}_c^T \boldsymbol{\mu}_c \mathbf{T})_n &= 0, & \forall n \in D_c \\ (\mathbf{C}_c^T \boldsymbol{\rho} \mathbf{C}_c \mathbf{T})_e + i\omega (\boldsymbol{\mu}_c (\mathbf{T} + \mathbf{G}_c \boldsymbol{\Omega}_c))_e &= 0, & \forall e \in D_c. \end{aligned} \quad (7)$$

The system (7) is singular and, to solve it, a conjugate gradient method without gauge condition is used.

III. DISCRETE PERTURBATION METHOD FOR $T - \boldsymbol{\Omega}$

Let us suppose that the presence of a defect in the conductive domain D_c , corresponds to a perturbation of its resistivity. To this aim we modify the resistivity of a tetrahedron $v_k \in D_c$ from ρ to $\rho + \rho^p$, where ρ^p is a perturbation of the resistivity. Correspondingly, we modify the constitutive matrix from $\boldsymbol{\rho}$ to $\boldsymbol{\rho} + \boldsymbol{\rho}^p$.

From (6b), the e.m.f. associated with dual edge $e_B \in v_k$ in the undefected configuration is $(\mathbf{U}_c)_{e_B} = (\boldsymbol{\rho} \mathbf{I})_{e_B}$, where \mathbf{I} is the array of eddy currents in D_c when the resistivity in D_c is ρ . It can be equivalently rewritten as

$$\begin{aligned} (\mathbf{U}_c)_{e_B} &= ((\boldsymbol{\rho} + \boldsymbol{\rho}^p) \mathbf{I} - \boldsymbol{\rho}^p \mathbf{I})_{e_B} \\ &= ((\boldsymbol{\rho} + \boldsymbol{\rho}^p) \mathbf{I} + \mathbf{U}_g)_{e_B} \end{aligned} \quad (8)$$

where, using (3) for \mathbf{I} , the term

$$\mathbf{U}_g = -\boldsymbol{\rho}^p \mathbf{I} = -\boldsymbol{\rho}^p \mathbf{C}_c \mathbf{T} \quad (9)$$

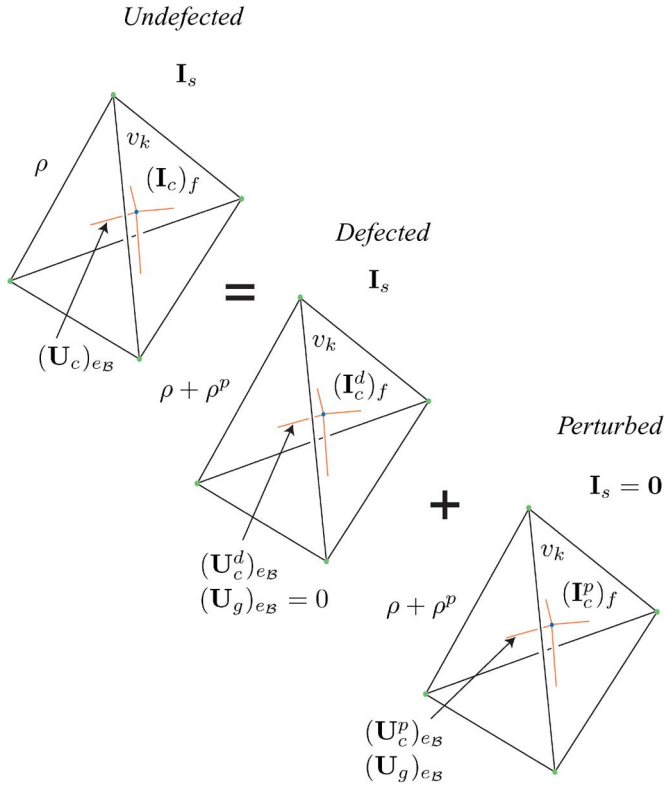


Fig. 2. The superposition for the tetrahedron v_k : the defected and perturbed configurations yield the undeformed configuration.

can be interpreted as an array \mathbf{U}_g of compensation e.m.f. generators $(\mathbf{U}_g)_{e_B}$ connected in series to each dual edge e_B of v_k .

Next, by applying the superposition of effects, we consider the following pair of configurations labeled with a superscript d to denote the defected configuration or p to denote the perturbed configuration, Fig. 2:

- The source currents array \mathbf{I}_s is active, the compensation e.m.f.s array \mathbf{U}_g is switched off. This is the defected configuration, where the resistivity in v_k is $\rho + \rho^p$ and the eddy currents \mathbf{I}^d account for the presence of the defect; From (9), we have that

$$\mathbf{U}_c^d = (\rho + \rho^p)\mathbf{I}^d$$

holds, where \mathbf{U}_c^d is the array of e.m.f.s in this configuration.

- The source currents array \mathbf{I}_s is switched off, the compensation e.m.f.s array \mathbf{U}_g is active. This is the perturbed configuration, where

$$\mathbf{U}_c^p = (\rho + \rho^p)\mathbf{I}^p + \mathbf{U}_g$$

holds. The sources are represented by \mathbf{U}_c^p given by (9) and \mathbf{U}^p , \mathbf{I}^p are the arrays of e.m.f.s and currents in this configuration.

A. Analysis of the Perturbed Configuration

From the above described superposition of effects, Fig. 2, the e.m.f.s and currents arrays \mathbf{U}_c^p , \mathbf{I}_c^p computed from an eddy-current analysis of the perturbed configuration, coincides with the

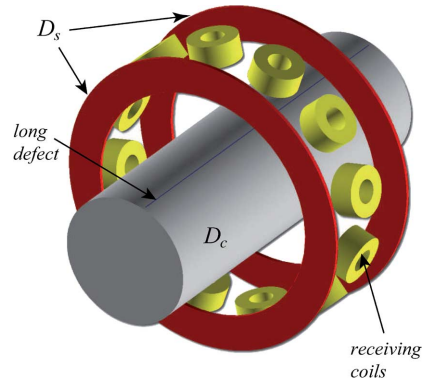


Fig. 3. Solid model of the entire geometry of the defect detection device.

opposite of the difference between e.m.f.s and currents arrays in the undeformed and defected configurations, yielding

$$\begin{aligned} \mathbf{U}_c^p &= -(\mathbf{U}_c - \mathbf{U}_c^d) \\ \mathbf{I}_c^p &= -(\mathbf{I}_c - \mathbf{I}_c^d). \end{aligned} \quad (10)$$

Now, we focus on the analysis of the perturbed configuration. We denote with D_d the subregion of D_c , where the defect is present and the resistivity of $v_k \in D_d$ has been modified with $\rho + \rho^p$. Along the dual edges of $e_B \in D_d$, we introduce the e.m.f. generators $(\mathbf{U}_g)_{e_B} = -(\rho^p \mathbf{C} \mathbf{T})_{e_B}$ in the (7) relative to the edges in D_c obtaining

$$\begin{aligned} (\mathbf{G}^T \boldsymbol{\mu} \mathbf{G} \boldsymbol{\Omega}^p)_n &= 0, & \forall n \in D_a \\ (\mathbf{G}^T \boldsymbol{\mu} \mathbf{G} \boldsymbol{\Omega}^p)_n &= 0, & \forall n \in D_s \\ (\mathbf{G}^T \boldsymbol{\mu} \mathbf{G} \boldsymbol{\Omega}^p)_n + (\mathbf{G}_c^T \boldsymbol{\mu}_c \mathbf{T}^p)_n &= 0, & \forall n \in D_c \\ (\mathbf{C}_c^T \rho \mathbf{C}_c \mathbf{T}^p)_e + i\omega (\boldsymbol{\mu}_c (\mathbf{T}^p + \mathbf{G}_c \boldsymbol{\Omega}_c^p))_e &= 0, & \forall e \in D_c - D_d \\ (\mathbf{C}_c^T (\rho + \rho^p) \mathbf{C}_c \mathbf{T}^p)_e + i\omega (\boldsymbol{\mu}_c (\mathbf{T}^p + \mathbf{G}_c \boldsymbol{\Omega}_c^p))_e &= -(\mathbf{C}_c^T \mathbf{U}_g)_e, & \forall e \in D_d. \end{aligned} \quad (11)$$

It must be noted that the array \mathbf{T} necessary to construct the term \mathbf{U}_g , has been computed from an independent analysis of the undeformed configuration. Often such an analysis can be quite simple by exploiting the symmetry of the undeformed configuration or it can be even performed as a one- or two-dimensional case.

IV. APPLICATION TO NONDESTRUCTIVE TESTING

The specific application describes the design of a device for the detection of long longitudinal defects that can be present during the hot mill rolling process of the steel bars with circular cross section, [11]. The bar consists of a conducting AISI 310 steel cylinder (34 mm of diameter, conductivity of $1.236 \cdot 10^6$ S/m and linear permeability coincident with μ_0), where a longitudinal perfectly insulating defect representing the D_d domain is assumed, 0.5 mm deep from the surface of the cylinder and 0.2 mm thick. The geometry of the problem is depicted in Figs. 3 and 4.

A pair of source coils (30 mm of inner radius, 39 mm of outer radius, 1 mm height, 7 turns each, 200 mA per turn, $f = 100$ kHz, counter series connected, 30 mm of axial distance between the coils) encircling the bar are considered and they represent the source region D_s . A set of 12 evenly spaced circular

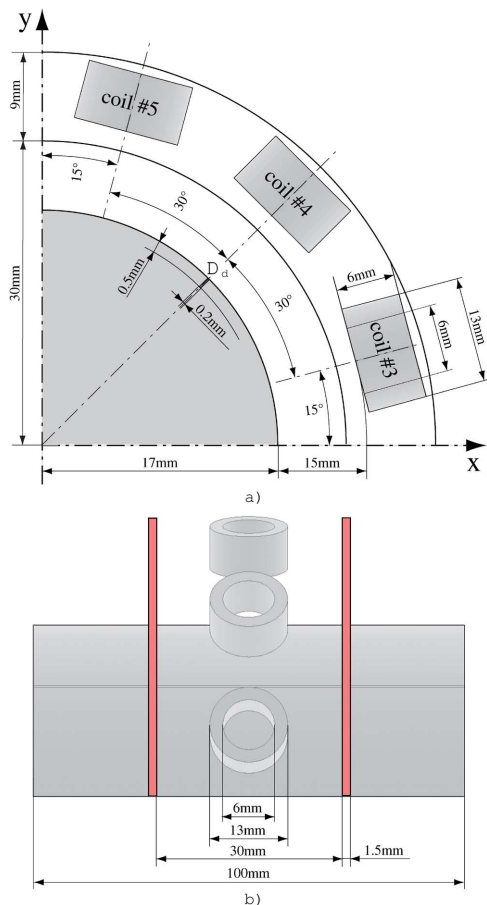


Fig. 4. Geometric data of one-quarter of the geometry concerning the device for defect detection: The 12 receiving coils are shown together with the pair of source coils encircling the bar with circular cross section.

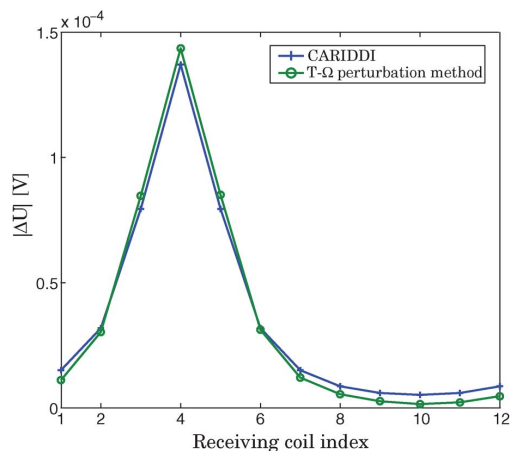


Fig. 5. Numerical comparison in terms of induced e.m.f. due to the defect over the receiving coils between the proposed formulation and an independent integral formulation (CARIDDI Code [2]).

coils (3 mm of inner radius, 6.5 mm outer radius, 6 mm height, 400 turns each) with axis directed as the radii of the bar, are considered in between the pair of source coils. The receiving coils will be placed close (not less than 15 mm) to an hot bar (about 1000°C); for this reason we deliberately avoided the use of magnetic cores since, it is well known, that magnetic materials like ferrites have a permeability strongly dependent with the temperature.

To have an estimate of the expected e.m.f. variations in the coils due to the presence of the defect, we computed the e.m.f. variations $\Delta U_k = U_k^d - U_k$ between the e.m.f. on the k -th coil in the defected configuration U_k^d and in the undefected one U_k , by means of the discrete perturbation method, Fig. 5.

A mesh consisting of about 1 million of tetrahedra is used for the computations, both for the undefected and the perturbed configurations; the solution of the final linear system of equations required about 160 s of CPU time on a laptop PC with 4 Gb of RAM, 2.4 GHz. The choice of tetrahedra is natural when curved domains have to be discretized. Moreover, a tetrahedra mesh is necessary in our geometry, since we have to model also the case of a cylinder with tilted axis, where an extruded hexahedral mesh is not possible. Of course our geometric perturbation approach remains valid also for a primal grid based on polyhedra. The value of the perturbation in the induced e.m.f.s over the receiving coils due to the defect calculated with the proposed formulation is compared (Fig. 5) to the ones computed with the CARIDDI code [2], [12], which implements an integral formulation.

V. CONCLUSION

The perturbation method, reducing the cancellation error, produces accurate results also for small variations in the solution. This is especially required when the tool is used as a forward solver for an inverse problem. Moreover, the method yields also to a considerable speedup. The mesh used in the perturbed problem may be reduced [1], considering only a limited region surrounding the defect, at a small fraction of the initial mesh.

REFERENCES

- [1] R. V. Sabariego and P. Dular, "A perturbation approach for the modeling of eddy current nondestructive testing problems with differential probes," *IEEE Tran. Magn.*, vol. 43, no. 4, pp. 1289–1292, Apr. 2007.
- [2] R. Albanese, G. Rubinacci, and F. Villone, "An integral computational model for crack simulation and detection via eddy currents," *J. Comput. Phys.*, vol. 152, pp. 736–755, 1999.
- [3] A. Bossavit and L. Kettunen, "Yee-like schemes on staggered cellular grids: A synthesis between FIT and FEM approaches," *IEEE Trans. Magn.*, vol. 36, no. 4, pp. 861–867, Jul. 2000.
- [4] T. Weiland, "A discretization method for the solution of Maxwell's equations for six-component fields," *Electron. Commun. (AEÜ)*, vol. 31, no. 3, p. 116, 1977.
- [5] E. Tonti, "On the geometrical structure of electromagnetism," in *Gravitation, Electromagnetism and Geometrical Structures*. Bologna, Italy: Pitagora Editrice, 1995, pp. 281–308.
- [6] E. Tonti, "Finite formulation of the electromagnetic field," *IEEE Trans. Mag.*, vol. 38, no. 2, pp. 333–336, Mar. 2002.
- [7] R. Specogna and F. Trevisan, "Eddy-currents computation with $T - \Omega$ discrete geometric formulation for a NDE problem," *IEEE Trans. Magn.*, vol. 44, no. 6, pp. 698–701, Jun. 2008.
- [8] R. Specogna, S. Suuriniemi, and F. Trevisan, "Geometric $T - \Omega$ approach to solve eddy-currents coupled to electric circuits," *Int. J. Num. Meth. Eng.*, vol. 74, no. 1, pp. 101–115, 2008.
- [9] P. Dlotko, R. Specogna, and F. Trevisan, "Automatic generation of cuts on large-sized meshes for the $T - \Omega$ geometric eddy-current formulation," *Comput. Methods Appl. Mech. Eng.*, vol. 198, pp. 3765–3781, 2009.
- [10] L. Codecasa, R. Specogna, and F. Trevisan, "Symmetric positive-definite constitutive matrices for discrete eddy-current problems," *IEEE Trans. Magn.*, vol. 43, no. 2, pp. 510–515, Feb. 2007.
- [11] R. Specogna and F. Trevisan, "Advanced geometric formulations for the design of a long defects detection system," *Nondestructive Testing and Evaluation*, vol. 24, no. 1, pp. 192–207, 2009.
- [12] R. Albanese and G. Rubinacci, "Integral formulation for 3D eddy current computation using edge elements," *IEE Proc. 135*, no. 5, pp. 457–462, 1988.